

REPLACEMENT OF THE SINGLE-PASS BPM SYSTEM WITH MicroTCA.4-BASED VERSATILE ELECTRONICS AT SPring-8

H. Maesaka^{*1}, RIKEN SPring-8 Center, Sayo, Hyogo, Japan

H. Dewa, T. Fujita, M. Masaki, N. Hosoda², S. Takano², JASRI, Sayo, Hyogo, Japan

¹also at JASRI, Sayo, Hyogo, Japan

²also at RIKEN SPring-8 Center, Sayo, Hyogo, Japan

Abstract

We have developed a versatile BPM readout electronics based on the MicroTCA.4 (MTCA.4) platform for the SPring-8 upgrade project, SPring-8-II. The new electronics are comprised of an RF frontend rear transition module (RTM) and a high-speed digitizer advance mezzanine card (AMC) having 10-channel, 16-bit, and 370 MSPS ADC. The field-programmable gate array (FPGA) on the AMC calculates both single-pass (SP) and closed-orbit distortion (COD) beam positions. The current BPM system at SPring-8 consists of approximately twenty SP-dedicated BPMs and more than 250 COD-dedicated ones. In advance of SPring-8-II, so far, we replaced half of the old SP BPM electronics with the new MTCA.4 ones and the rest of the old SP BPM electronics are being renewed this summer. The SP resolution of the new BPM electronics was confirmed to be better than 100 μm for a 0.1 nC single bunch, sufficient for SPring-8-II. The new BPM electronics were applied to regular tuning items, such as the adjustment of kicker magnets for pulsed orbit bumps in the beam injection, and the functionalities were confirmed to be compatible with the old SP BPM system. Thus, the MTCA.4-based BPM electronics are ready for SPring-8-II.

INTRODUCTION

The low-emittance upgrade of the SPring-8 storage ring, SPring-8-II [1] was proposed, and many new accelerator components have been developed. The natural emittance will be squeezed from 2.4 nm rad to 100 pm rad by reducing the beam energy from 8 GeV to 6 GeV and by using a 5-bend achromat lattice (5BA).

A new BPM system for SPring-8-II was also developed. The single-pass (SP) BPM resolution is required to be 100 μm std. for a 0.1 nC injected bunch. The error on the electrical center should be within $\pm 100 \mu\text{m}$ before the beam-based calibration. The closed-orbit distortion (COD) BPM is demanded to be sufficiently stable within 5 μm peak-to-peak for 1 month. To fulfill these requirements, we studied the following BPM components:

1. Button BPM electrodes made of molybdenum [2].
2. Radiation-tolerant coaxial cables.
3. BPM readout electronics based on MicroTCA.4 (MTCA.4) [3].

* maesaka@spring8.or.jp

Since the new electronics will benefit the operation of the current SPring-8 storage ring, replacement of the BPM electronics was scheduled in advance of the actual upgrade work. The SPring-8 storage ring has 48 cells (44 double-bend cells and 4 long straight ones). There are typically 6 BPMs in each cell and approximately 280 BPMs in total. Before the development of the new MTCA.4-based electronics, the existing BPM system has two types of readout electronics, COD BPM and SP BPM, and typically one BPM out of 12 (6 BPMs \times 2 cells) is processed by SP BPM and the other 11 are precessed by COD BPM. Contrary to the old electronics, the new MTCA.4-based electronics have both SP BPM and COD BPM functions. Therefore, both SP BPM and COD BPM can be replaced with the MTCA.4 electronics. Since the SP BPM system is more than 25 years old and hard to maintain, we decided to replace the SP BPM electronics with the MTCA.4 ones in advance of the COD BPM. The COD BPM system will be upgraded to MTCA.4 in the actual SPring-8 upgrade work.

The new electronics were first installed into the current SPring-8 ring to implement the adaptive feed-forward correction (AFC) of the error kick from the fast helicity switching beamline [4] in 2019. Old SP BPMs connected to the four BPM heads connected to the four BPM heads selected for the AFC were replaced with the MTCA.4 at that time. Another ten units of SP BPMs were then upgraded to MTCA.4 in 2021 and the rest of the SP BPM units are being replaced in this summer shutdown period (2023).

We describe the design of the MTCA.4-based BPM electronics and introduce the software for data taking. The basic performance of the SP BPM function is presented and compared with the old SP BPMs.

MTCA.4-BASED ELECTRONICS

A block diagram of the MTCA.4-based electronics is illustrated in Fig. 1. The signal from each BPM electrode is fed into the BPM rear transition module (RTM). The signal is filtered by a band-pass filter at the accelerator frequency of 508.58 MHz and the signal level is adjusted by step attenuators and low-noise RF amplifiers. The signal is then converted to a balanced differential signal by a BALUN since the ADC on the digitizer advanced mezzanine card (AMC) receives a differential balanced signal. The digitizer AMC has 10 ADC channels and hence one board can process signals from two BPMs. The ADC has a 16-bit resolution and a maximum sampling rate of 370 MHz. Since the signal frequency is higher than the Nyquist frequency of the ADC,

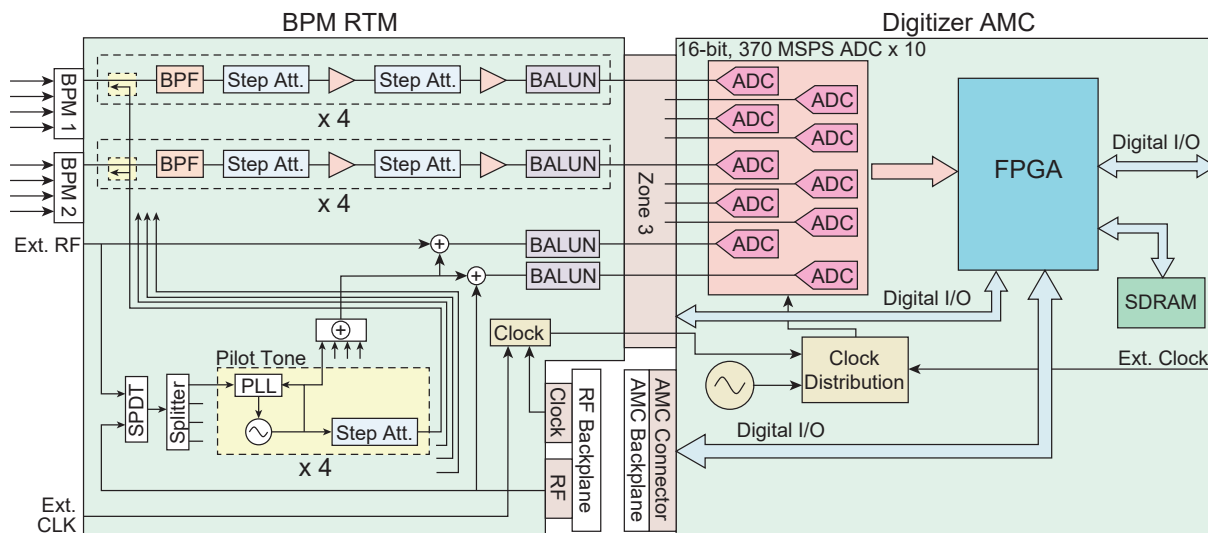


Figure 1: Block diagram of the readout electronics.

the signal is detected by an under-sampling scheme. The actual sampling frequency was set to 363.27 MHz, corresponding to 5/7 of the acceleration frequency. In this case, the waveform taken by the ADC looks like an intermediate frequency (IF) signal having 145.31 MHz. This IF signal is digitally converted to an IQ (In-phase and Quadrature) baseband signal and the amplitude and phase are calculated. The differential over summation (Δ/Σ) of the amplitudes of the four electrodes is calculated, and the beam position is obtained from a polynomial function.

To correct gain drifts etc. of the electronics, the RTM is equipped with a 4-channel pilot tone generator. Each pilot tone generator is connected to each electrode of a BPM.

In the FPGA, both SP BPM and COD BPM are processed in parallel. The SP BPM logic masks the period without any beam signal and integrates input signal power for each turn. The COD-BPM logic decimates the IQ signal to the three data rates, the revolution frequency of 209 kHz (Turn-by-Turn), 10 kHz (Fast Acquisition, FA), and 10 Hz (Slow Acquisition, SA). The Δ/Σ for each signal stream is calculated, and the beam position is computed by a 7th-order polynomial. These data are stored in the RAM on the digitizer AMC and then transferred to the CPU via a PCI-express bus.

The injection timing signal for the SP BPM trigger etc. is distributed by MTCA.4 trigger modules [5] from the SACLA linear accelerator [6]. The trigger module in the BPM system receives the trigger signal from SACLA and transmits the data acquisition trigger to the digitizer AMC via the AMC backplane.

SOFTWARE

The digitizer AMC is controlled by an MTCA.4 CPU module, where the operating system of Ubuntu 16.04 is running. The BPM system is controlled from an operating console by an MQTT messaging system, and the BPM data are taken by the MDAQ framework [7]. All the SA COD BPM data

are stored in the event-synchronized database with a data rate of 10 Hz. The other COD BPM data (TbT and FA) and SP BPM data are dumped into data files on request.

Since the SP BPM data needs some timing adjustments before data taking, we developed a graphical user interface (GUI) of SP BPM for convenient data acquisition. A screenshot of the SP BPM GUI is shown in Fig. 2. By using this, we can adjust the revolution trigger timing to the bunch timing from the raw signal amplitude waveforms and then set the injection trigger timing to the first turn of the plot. After the timing adjustment, SP BPM data at an injection trigger can be easily obtained and plotted.

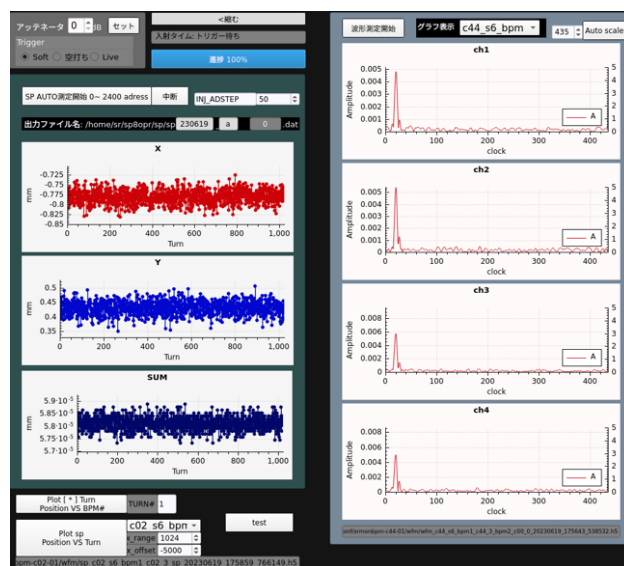


Figure 2: Screenshot of the SP BPM GUI. Horizontal and vertical positions and sum value for each turn are plotted in the left figures, along with some control widgets. The raw signal amplitude waveform for each electrode is shown in the right figures.

SP BPM DATA

Injected Beam

An example of SP BPM data from one BPM is plotted in Fig. 3, where a single bunch of approximately 0.2 nC was injected. The sum amplitude is promptly increased at the first turn and almost constant after injection. Since the injected beam is horizontally offset from the beam orbit, a large betatron oscillation was excited in the first few hundred turns. A synchrotron oscillation with a period of about 100 turns is also observed due to a finite horizontal dispersion and errors in energy and timing of the injected bunch. The

vertical position data shows small but finite betatron and synchrotron oscillations due to an offset of the beam orbit of the injected bunch and dispersion leakage to the vertical direction. Since the sum signal is calculated by a vector sum of complex amplitude of the four electrodes, the beam arrival phase with respect to the reference RF signal can be also obtained, as shown in the bottom plot of Fig. 3. The synchrotron oscillation is observed in the phase of the sum signal as well, but the oscillation phase is $\pi/2$ shifted from that of the position data. This phase shift is consistent with the time evolution of electrons in the longitudinal phase space.

Position Resolution

The position resolution was evaluated by kicking a stored single bunch with kicker magnets to make a pulsed orbit bump for beam injection. The stored current was approximately 0.1 mA, corresponding to 0.5 nC, and the amplitude of the betatron oscillation was approximately 0.4 mm. SP BPM data from 7 BPMs were taken in this measurement. We compared the beam position of one BPM with the prediction from the other 6 BPMs. Figure 4 shows a scatter plot of the horizontal beam position at a specified BPM vs. the prediction from the other BPMs. The standard deviation of the difference between data and prediction for each BPM is thought to be the position resolution. The horizontal position resolution was evaluated to be approximately 17 μm for an electron bunch with 0.5 nC, as plotted in Fig. 5. When the bunch charge is reduced to 1/5 (0.1 nC), the position resolution will be 5 times larger than this value. Even in this situation, the resolution is still below 100 μm and enough for single-pass measurements in SPring-8-II. Since the size of the SPring-8-II vacuum chamber will be smaller than that of

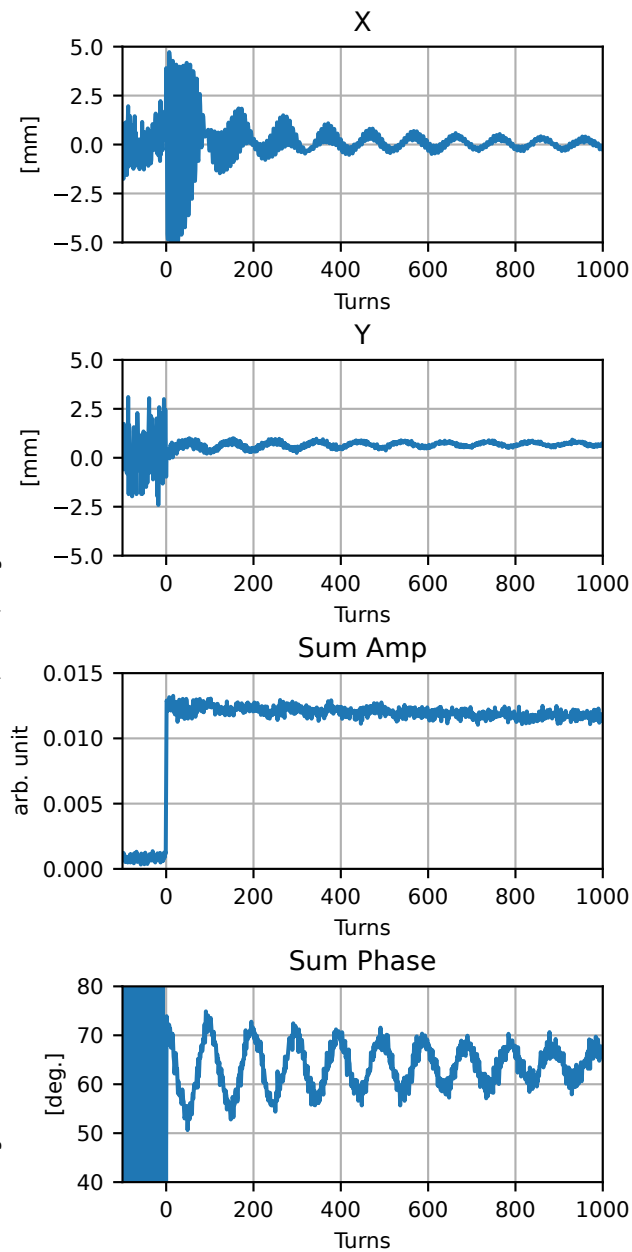


Figure 3: Example of SP BPM data from one BPM at beam injection. Horizontal and vertical beam positions, sum amplitude, and sum phase are shown from top to bottom.

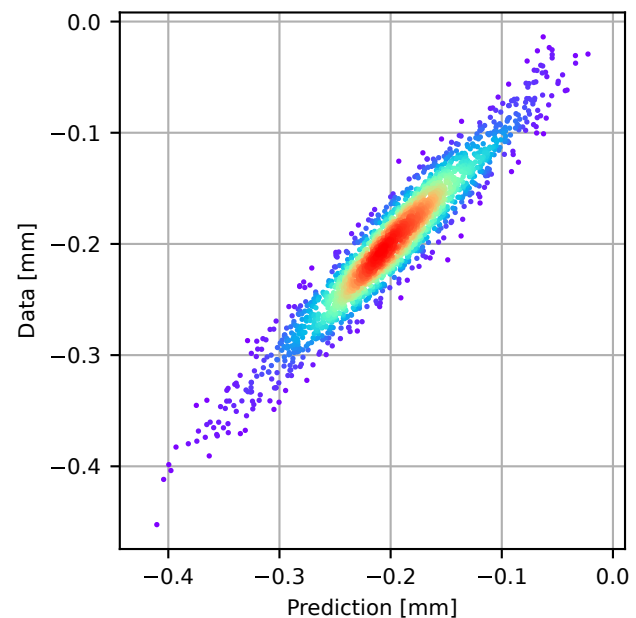


Figure 4: Comparison between the horizontal beam position at a BPM and the prediction from other BPMs.

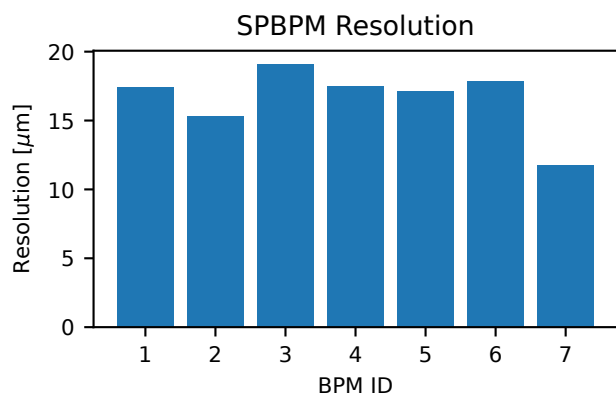


Figure 5: Horizontal SP BPM resolution of 7 BPMs.

the current SPring-8 ring, the SP BPM resolution is expected to be better than this measurement.

Injection Orbit Bump Adjustment

The current SPring-8 storage ring makes a pulsed orbit bump with four dipole kicker magnets for the off-axis beam injection. Since it is important to close the orbit bump as perfectly as possible with matched kicker waveforms so as not to affect the stored beam, adjustment of the dipole kickers is necessary at the beginning of each operation cycle [8]. The kicker magnets used to be adjusted by using the data from the old SP BPM system so that the oscillation of the stored beam is minimized. The same adjustment procedure should work well with the new MTCA.4-based BPM system.

Therefore, we measured the orbit oscillation caused by the kicker magnets with both old and new SP BPM systems to confirm that both data were consistent with each other. The SP BPM data were taken by shifting the kicker magnet timing every 50 RF buckets (98 ns), and the orbit oscillation amplitude due to the residual kick of the kicker magnets for each bunch address was evaluated. Figure 6 shows the RMS of the beam positions at the used SP BPMs as a function of the bunch address. The difference in the os-

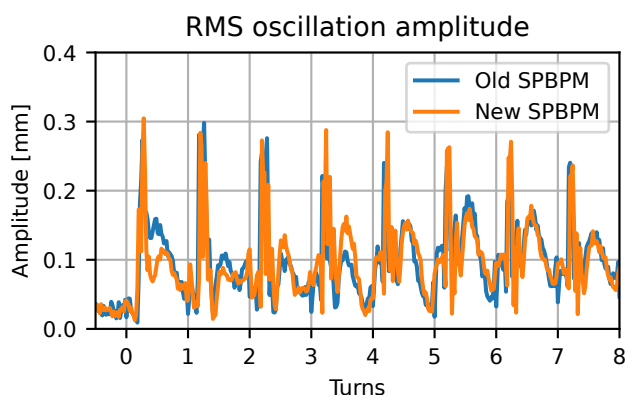


Figure 6: RMS amplitude of the orbit oscillation by the residual kick of the kicker magnets. The blue (orange) line shows the data from the old (new) SP BPM. The horizontal axis shows the bunch timing with respect to the bump pulse timing.

cillation amplitude data between the old and new SP BPMs was small enough (less than 0.1 mm). Consequently, the new MTCA.4 SP BPM system is ready for the tuning of the current SPring-8 storage ring.

SUMMARY

For the next-generation hard X-ray light source project, SPring-8-II, we developed MTCA.4-based versatile BPM readout electronics. Since the new electronics are applicable to the current SPring-8, we decided to first replace the old SP BPM electronics with the new ones. After finishing the replacement of half of the SP BPM by 2021, we are now upgrading the remaining half this summer. The SP BPM performance of the MTCA.4 electronics were evaluated, and confirmed to be sufficient for both SPring-8 and SPring-8-II. The trajectory of an injected electron beam was appropriately observed. The SP BPM resolution was obtained to be 17 μm for a 0.5 nC single-bunch. The beam oscillation caused by the residual kick of the injection orbit bump was compared between the old and new electronics, and confirmed to be consistent with each other. Thus, the MTCA.4-based BPM electronics are ready for SPring-8-II, and the upgrade work of the BPM system is expected to be smoothly carried out by replacing the readout electronics in advance.

REFERENCES

- [1] SPring-8-II Conceptual Design Report, Nov. 2014. <http://rsc.riken.jp/pdf/SPring-8-II.pdf>
- [2] M. Masaki *et al.*, “Design Optimization of Button-type BPM Electrode for the SPring-8 Upgrade”, in *Proc. IBIC'16*, Barcelona, Spain, Sep. 2016, pp. 360–363. doi:10.18429/JACoW-IBIC2016-TUPG18
- [3] H. Maesaka *et al.*, “Development of MTCA.4-based BPM Electronics for SPring-8 Upgrade”, in *Proc. IBIC'19*, Malmö, Sweden, Sep. 2019, pp. 471–474. doi:10.18429/JACoW-IBIC2019-WEB003
- [4] M. Masaki *et al.*, “Adaptive feedforward control of closed orbit distortion caused by fast helicity-switching undulators”, *J. Synchrotron Rad.*, vol. 28, pp. 1758–1768, 2021. doi:10.1107/S160057752101047X
- [5] H. Maesaka *et al.*, “Development of a Trigger Distribution System Based on MicroTCA.4”, in *Proc. IPAC'22*, Bangkok, Thailand, Jun. 2022, pp. 1171–1173. doi:10.18429/JACoW-IPAC2022-TUPOPT067
- [6] H. Maesaka *et al.*, “Full Energy On-Demand Beam Injection from SACLA to SPring-8 Storage Ring”, in *Proc. IPAC'21*, Campinas, Brazil, May 2021 pp. 4508–4513. doi:10.18429/JACoW-IPAC2021-FRXA01
- [7] T. Sugimoto *et al.*, “Status of the control system for fully integrated SACLA/SPring-8 accelerator complex and new 3 GeV light source being constructed at Tohoku, Japan”, in *Proc. ICALEPCS'19*, New York, USA, Oct. 2019, pp. 904–908. doi:10.18429/JACoW-ICALEPCS2019-WECPL01
- [8] T. Ohshima *et al.*, “Suppression of Stored Beam Oscillation Excited by Beam Injection”, in *Proc. EPAC'04*, Lucerne, Switzerland, Jul. 2004, MOPKF047, pp. 414–416.